Metallurgical and Materials Engineering *Research paper*
Association of Metallurgical Engineers of Serbia AMES *https://doi.org/10.30544/738*

EXPERIMENTAL INVESTIGATION ON IMPACT ENERGY OF FRICTION STIR WELDED ALUMINUM AND COPPER DISSIMILAR JOINT USING FULL FACTORIAL METHOD

Gurunath Shinde[1, 2], Rachayya Arakerimath[1]*

[1]Department of Mechanical Engineering, G.H.Raisoni College of Engg. And Mgmt., Pune, India
[2]Department of Mechanical Engineering, Dr. Daulatrao Aher College of Engineering, Karad, India

Received 22.09.2021
Accepted 26.03.2022

Abstract

This research work carried out friction stir welding (FSW) of dissimilar aluminum AA3003-H12 and copper C12200-H01, with wide application in the refrigeration and heat exchanger industry. The main aim of this study is to investigate the influence of process parameters, i.e. pin type (PT), weld speed (WS), rotational speed (RPM), and shoulder diameter (SD) on impact energy (IE) of Al-Cu welded joint. The experimental study used the full factorial method with mixed levels of process parameters. Analysis of Variance (ANOVA) determines the significance of process parameters on impact energy. The results of the analysis of variance (ANOVA) shows that rotational speed (RPM) is the most influential process parameter contributing to the impact energy (IE) of dissimilar Al-Cu weld joint. The response optimizer tool in Minitab 18 software gives optimum weld conditions of process parameters for better weld performance. The FSW experiment with a tapered pin, weld speed of 16 mm/min, rotational speed of 1120 rpm, and shoulder diameter of 22.5 mm obtained the maximum impact energy value of 6.5367 J. The fine-grain recrystallization formed intermetallic compounds in the stir zone (SZ). These intermetallic compounds give a maximum microhardness of 382.24 $Hv_{(0.1)}$. The microstructure analysis of the stir zone (SZ) shows an equiaxed grain structure on the Cu side, while the Al side shows a fine recrystallized grain structure.

Keywords: friction stir welding; aluminum-copper; impact energy; full factorial analysis.

*Corresponding author: Gurunath Shinde, *gurunathshinde@yahoo.com*

Introduction

Dissimilar joining, i.e. aluminum and copper, is challenging due to the difference in physical properties of both materials. The welding of dissimilar Al-Cu has wide applications in the fabrication and construction of various equipment in the electrical and electronics, chemical, refrigeration, and heat exchanger industry. The successful joining of dissimilar Al-Cu depends upon proper material mixing. 'Friction stir welding is a solid-state method of joining various similar and dissimilar materials i.e. aluminum, copper, and steel'. Cam et al discussed advances and recent developments in FSW and FSSW of Al alloys. The effect of higher strength interlayer and external cooling on the properties of friction stir welded AA6061-T6 joints is studied. The mechanical properties with microstructural analysis of FSW of 63% Cu-37% Zn brass, St 37, St 44 steel, and St 52 steel are also explained.

Friction stir welding was originally developed for joining Al-alloys is a solid-state method of joining various similar and dissimilar materials i.e. aluminum, copper, and steel' [1-6]. Friction stir welding employs a rotating tool with the small probe attached to the shoulder plunged into the materials under axial pressure. The friction produced between the tool shoulder and materials causes plasticization and material softening. The stirring action provides uniform material mixing, which gives a solid weld bond on cooling [7]. *Ashok Raj J.* [8] carried out a literature study of friction stir welding of dissimilar aluminum and copper to reveal insights into the successful joining of dissimilar materials. This literature review investigates the effects of different process parameters on weld characterization, material flow pattern, tool geometry, defects formation, thermal distribution, etc. *Winarto et al.* [9] explained friction stir welding of dissimilar aluminum AA 5052 and pure copper. Their results indicate that different pin tool geometry influences weld microstructure, grain size, and Al-Cu intermetallic compound formation. The formation of varying structures influenced the mechanical properties of weld joints. *Mehta et al.* [10] concluded that the cylindrical pin tool is more suitable than the tapered pin tool for welding aluminum AA6061-T6 and copper ETP-Cu, due to the uniform mixing of Al-Cu. The presence of Al-Cu intermetallic compounds makes the weld zone more brittle and increases hardness values. Shoulder diameter and tilt angle are the significant parameters for plunge load. *Sharma et al.* [11] showed that cylindrical and square pin profile produces a defect less weld joint between AA5754 and Cu, due to better stirring assisted pulsating action. More stirring on the soft Al side shows clear flow lines in the stir zone. Square tool pin profile shows better joint and microhardness than tool pin profiles.

Shankar et al. [12] discussed the successful aluminum AA1050 and oxygen-free copper fabrication. The highest tensile strength obtained was 91% of AA1050. The weld speed and tool offset significantly affect the mechanical property of weld joints. Sufficient heat input is required for proper material mixing of Al-Cu. Heat input is a function of process parameters, i.e. pin type, rotational speed, weld speed, shoulder diameter, etc. Mechanical properties of Al-Cu weld joint such as impact energy depends upon proper Al-Cu material flow in the weld joint. Friction stir welding uses a rotating tool with a small pin of different shapes, which plunges into the joining materials and travels along the weld line [13]. *Chen et al.* [14] studied the influence of process parameters, i.e. rotational speed, weld speed, tilt angle, and pin tool diameter, on the impact value of dissimilar AA6061 aluminum and SS400 low carbon steel. The most influencing process parameters affecting impact strength are rotational speed and weld speed. Low rotational

speed and weld speed achieve better impact strength of weld joint. *Safeen et al.* [15] investigated various weld properties, i.e. tensile strength, impact toughness, and hardness of weld joining of aluminum AA6061-T6.The influence of process parameters, i.e. rotational speed, weld speed, tilt angle, and pin profile using response surface methodology (RSM) with central composite design (CCD). The tool pin profile is the most influencing process parameter to achieve better weld properties. The FSW tool with a simple cylindrical pin gives better ultimate tensile strength, impact toughness, and microhardness. A cylindrical pin achieved maximum ultimate tensile strength, impact toughness, and microhardness, the rotational speed of 1150 rpm, weld speed of 70 mm/min, and a tilt angle of 3^0. The three experimental trials confirmed the results of optimum parameters.

Kumar et al. [16] explained the mechanical behavior of dissimilar AA6063 and AA5083 aluminum alloys during friction stir welding. The experimental study used the rotational speed of 600, 800, and 1000 rpm at a constant weld speed of 40 mm/min and an axial load of 4 kN for experimental trials. The FSW trial with a low rotational speed of 600 rpm produced the maximum impact strength. The increase in rotational speed decreases impact strength. *Nia et al.* [17] performed joining of the copper workpiece with the rotational speeds of 500, and 700 rpm at weld speeds of 56, and 112 mm/min using a simple threaded cylindrical pin tool. The FSW with a double pass, rotational speed at 500 rpm, and 56 mm/min weld speed gives the highest impact strength. The grain size refinement in the reoccurrence of re-crystallization achieved this highest value of impact strength. The base metal shows a reduction in grain size up to 86.1%. Therefore, the smaller grain size obtained the highest value of impact strength. *Lakshminarayanan et al.* [18] revealed microstructure, tensile strength, and impact toughness of friction stir welding of AISI 1018 mild steel. The rotational speed of 1000 rpm and welding speed of 50 mm/min performed the joining of materials. Tensile strength and hardness were recorded at 8% more than the base metal due to the formation of fine equiaxed ferrite and pearlite grains in the stir zone. The decrease in ductility and impact toughness is seen as compared with the base material having tungsten particles in the stir zone.

Karthick et al. [19] studied tensile strength, impact toughness, and microhardness of dissimilar welding of steel (modified 9 Cr-1Mo ferritic) and stainless steel (316LN austenitic). The study carried out the impact toughness of various regions of dissimilar joints. The Inconel 182 buttering region's impact toughness values were lowest than other regions, whereas all other impact toughness values are higher than the minimum prescribed values. *Zhou et al.* [20] evaluated the influence of welding speed on the impact toughness of weld joints of titanium alloy at room temperature. The weld joint found an impact toughness value 50 % more than parent metals. Improved impact toughness properties are due to the reduced primary α grains in the weld zone. *Qinglei et al.* [21] investigated the influence of different welding wires on the characterization of strength and toughness of Q550 steel welded joint. The heat-affected zone observed the highest impact absorption energy while the lowest was in the fusion zone. The MKG60-1 wire found higher impact toughness values of base metal and weld joint than the ER50-6 wire. *Chiong et al.* [22] explained the influence of process parameters on weld performance of AISI1018 low carbon weld joints. The variation in the absorbed impact energy is due to the poor weld quality. The maximum impact value was 86J due to the high-absorbed impact energy leading to lesser weld defects. The slag in the weld zone produces a minimum impact value of 44J.

Choudhari et al. [23] observed the influence of the water-cooled submerged arc welding process on chemical composition and impact toughness of AISI 1023 weld joining. The results obtained reveal that a high preheat current decreases the heat-affected zone and improves impact toughness due to grain refinement. Fractography of fracture of weld joints shows the fine structure at high preheat current. *Yayla et al.* [24] used different welding processes to study the influence method for the joining of HY 80 steel. Different mechanical properties, i.e. tensile strength, impact toughness, and hardness, analyses were conducted in the temperature range of -20^0C to 20^0C. The impact test shows that higher heat input in SAW and SMAW weld joints gives better HAZ impact toughness than the GMAW process, in the temperature range. *Das et al.* [25] investigated impact energy during the joining of different aluminum AA6106-T6 and AA6351-T6 using friction stir welding. The weld properties indicated the substantial variation in the behavior of impact strength. The fracture pattern of the impact test sample shows ductile fibrous nature in SEM analysis.

Balaguru et al. [26] discussed the influence of weld composition on the impact toughness of shielded metal arc welded ultra-high hard armor steel joints. The amount of ferrite in weld metal has an inverse effect on the impact toughness of weld joints. *Krishna et al.* [27] explained the effect of friction stir welding on mechanical properties of dissimilar joining of aluminum AA2024 and AA7075. The weld joint with the rotational speed of 1120 rpm and the square pin tool gave maximum impact energy of 9J. *Verma et al.* [28] studied the joining of dissimilar Mg-AZ31B and Al-AA6061 with friction stir welding. The average rotational speed and lower traverse speed due to soft Al patches showed higher impact energy. *Shinde et al.* [29] studied the effect of friction stir welding of dissimilar aluminum AA3003-H12 with copper C12200-H01 on various weld performances such as UTS, % E, and YS. This study extends to the analysis of maximum impact energy with microstructural analysis and microhardness measurement. There are no previous studies in the open literature investigating the effect of the friction stir welding process on the impact energy of dissimilar friction stir welded aluminum AA3003-H12/Copper C12200-H01 joint. The dissimilar joining of aluminum AA3003-H12 and copper C12200-H01 has wide commercial application in the refrigeration and heat exchanger industry.

Materials and Methods

Material data and experimental method

The friction stir welding process of Aluminum AA3003-H12 and Copper C12200-H01was carried out on a rigid HMT FN2 conventional milling machine with a 10 HP motor-powered spindle. Both materials prepared specimens of a length of 150 mm, a width of 75 mm, and a thickness of 2 mm to join the materials. Table 1 and Table 2 show the chemical composition of base metals AA3003-H12 and Copper C12200-H01.

Table 1. Chemical composition of Aluminum AA3003-H12.

Elements	Zn	Sn	S	P	Cr	Pb	Si	Mg	Fe	Cu	Ni	Mn	Al
wt.%	0.062	0.042	0.008	0.016	0.02	0.028	0.12	0.032	0.156	0.099	0.057	1.24	98.12

Table 2. Chemical composition of Copper C12200-H01.

Elements	Zn	Pb	Bi	P	Cu
wt.%	0.007	0.004	0.003	0.018	99.967

Fig. 1(a) shows friction stir welding set up with a rigid fixture for correctly positioning workpiece materials. This study used a non-consumable FSW tool of H13 tool steel with a cylindrical and tapered pin for experimental trials, as shown in Fig. 1(b) and Fig. 1(c). The FSW tool was machined and hardened up to 56 HRC to avoid tool failure and wear resistance. The constant tool offset of 0.75 mm to the Al side and tilt angle of 2^0 were used for this study. The specimens for the impact test are prepared as per the ASTM E 23-04 standard using wire EDM, as shown in Fig. 2. The diamond wheel cutting fabricated sample for microstructural analysis at the weld cross-section, followed by grinding and polishing coarse to fine grade emery papers (400, 600, 800, 1200). The velvet cloth polishing and cleaning gives a mirror finish. The Al side was etched with Keller's reagent, while the Cu side was etched with $FeCl_3$ (5 gm) + ethanol (10 ml) + HCl (10 ml) + distilled water (50 ml). The microstructure study analyzed different welding zones such as base metal (BM), heat-affected-zone (HAZ), thermo-mechanical-affected-zone (TMAZ), and stir zone (SZ). The microhardness measurement used 100 gm load at a dwell time of 10 seconds across the weld section on the middle layer of experiment no.21**.**The two indentations kept a distance of 1 mm. The 15 indentations on either side give a total of 30 indentations.

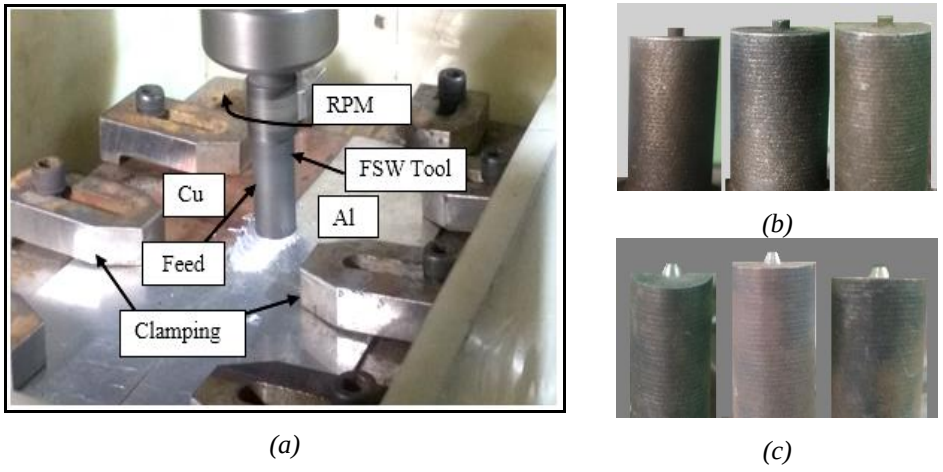

Fig. 1. FSW Experimental set-up (a) Setup with fixture (b) Cylindrical Pin tool (c) Tapered Pin tool.

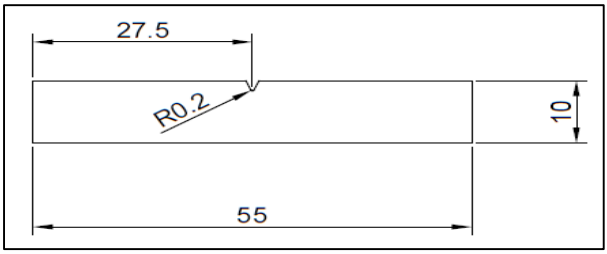

Fig. 2. Standard Impact Test Specimen in mm (ASTM E23-04).

Full Factorial Analysis

The literature study reviewed the final process parameters and levels in preliminary FSW trial experiments. Table 3 shows four influencing parameters and their respective levels. The Minitab 18 software established the design of the experiment with full factorial mixed orthogonal array L_{36}, as shown in Table 4.

Table 3. Factors with their levels.

Factors	Levels		
	1	2	3
Pin Type (PT)	Cylindrical	Tapered	-
Weld Speed (WS)	16 mm/min	20 mm/min	-
RPM	1120	1400	1800
Shoulder Dia. (SD)	17.5 mm	20 mm	22.5 mm

The three experiments for each combination gave average impact energy with standard deviation, as shown in Table 4. The impact-testing machine tested the impact energy on the impact test machine.

Results and discussions

The analysis of variance (ANOVA) determines the adequacy of the developed regression model, as shown in Table 5. The calculated value of F-ratios is higher than tabulated values of F-ratio at a 95% confidence level, so the developed regression model is adequate. The predicted results obtained by developed regression models will be sufficient when they are ideal matches with the experimental values (R^2~1). The R^2 value obtained for IE is 0.9732, which is close to one, as shown in Table 6. Hence, the developed regression model is adequate.

Table 4. FSW Trials using Full Factorial Method with Mixed Orthogonal Array (L_{36}).

DOE No	**Process Parameters**				**Impact Energy**	**Standard Deviation**
	Pin Type	***WS (mm/min)***	***RPM***	***SD (mm)***	***IE (J)***	***Std Dev***
1	1	16	1120	17.5	3.62	0.74
2	1	16	1120	20	4.78	1.25
3	1	16	1120	22.5	5.81	1.5
4	1	16	1400	17.5	2.26	0.5
5	1	16	1400	20	3.13	0.75
6	1	16	1400	22.5	3.49	1.24
7	1	16	1800	17.5	0.46	0.16
8	1	16	1800	20	0.62	0.14
9	1	16	1800	22.5	0.62	0.25
10	1	20	1120	17.5	1.42	1
11	1	20	1120	20	1.75	0.94
12	1	20	1120	22.5	2.75	1.2
13	1	20	1400	17.5	0.62	0.36
14	1	20	1400	20	1.09	0.48
15	1	20	1400	22.5	1.09	0.56
16	1	20	1800	17.5	0.30	0.08
17	1	20	1800	20	0.30	0.12
18	1	20	1800	22.5	0.46	0.16
19	2	16	1120	17.5	4.78	1.84
20	2	16	1120	20	5.84	1.68
21	2	16	1120	22.5	6.03	1.22
22	2	16	1400	17.5	1.26	0.42
23	2	16	1400	20	1.92	0.36
24	2	16	1400	22.5	2.09	1.04
25	2	16	1800	17.5	0.15	0.05
26	2	16	1800	20	0.46	0.28
27	2	16	1800	22.5	0.77	0.36
28	2	20	1120	17.5	1.92	0.92
29	2	20	1120	20	2.43	1.08
30	2	20	1120	22.5	5.17	1.80
31	2	20	1400	17.5	1.26	0.54
32	2	20	1400	20	1.42	0.36
33	2	20	1400	22.5	1.58	0.74
34	2	20	1800	17.5	0.46	0.16
35	2	20	1800	20	0.62	0.18
36	2	20	1800	22.5	0.93	0.04

Table 5. Analysis of Variance (ANOVA).

Source	DF	IE			
		Adj SS	Adj MS	F-Value	P-Value
Model	19	107.625	5.6645	30.61	0.000
Linear	6	89.539	14.9232	80.64	0.000
PT	1	0.565	0.5648	3.05	0.1
WS	1	14.075	14.0754	76.06	0.000
RPM	2	68.589	34.2947	185.32	0.000
SD	2	6.31	3.1549	17.05	0.000
2-Way Interactions	13	18.085	1.3912	7.52	0.000
PT*WS	1	1.559	1.5589	8.42	0.01
PT*RPM	2	2.904	1.4522	7.85	0.004
PT*SD	2	0.094	0.0471	0.25	0.778
WS*RPM	2	9.935	4.9677	26.84	0.000
WS*SD	2	0.336	0.1678	0.91	0.424
RPM*SD	4	3.257	0.8143	4.4	0.014
Error	16	2.961	0.1851		
Total	35	110.586			

Fig. 3 shows the normal probability plot of IE. It indicates that experimental results are close to the fitted line, which agrees with the regression models. The factors and their interaction exceeding the marked red line in Pareto charts are the most influencing factors, as shown in Fig. 4. The main effect plot shows the influence of various process parameters, i.e. pin type, weld speed, rotational speed, and shoulder diameter on impact energy as shown in Fig. 5. The most influencing factor contributing to the impact energy of weld is rotational speed (RPM). Optimum levels of process variables to obtain better values of response variables are obtained using the response optimizer tool in Minitab 18 software. Fig. 6 shows the optimization plots obtained using a response optimizer for impact energy. The response optimizer finds optimum process variables pin type, weld speed, rotational speed, and shoulder diameter to get maximum impact energy. It also calculates the response variable at the optimum level of process variables. The tapered pin, weld speed of 16 mm/min, rotational speed of 1120 rpm, and shoulder diameter of 22.5 mm shows a maximum IE of 6.5367 J. The influencing process parameter on impact energy can be determined using the value of the F-ratio. The most influencing process parameter on impact energy is rotational speed (RPM); with the highest F-ratio obtained by analysis of variance (ANOVA).

The contour maps in Minitab are useful to understand the influence of process parameters on the response function [30]. The contour map of the impact of significant to parameters such as rotational speed (RPM), welding speed (WS), and shoulder diameter (SD) on response function i.e. impact energy (IE) is shown in Fig. 7. Pin type (PT) is not s significant process parameter as it has a higher P-value of 0.1 which is more than 0.05. Fig. 7 (a) shows that impact energy (IE) decreases with the increase in rotational speed (RPM) when welding speed (WS) is constant and vice-a-versa. Fig. 7 (b) shows that impact energy (IE) decreases with the increase in rotational speed (RPM) when shoulder diameter (SD) is constant, while impact energy (IE) increases with the increase in shoulder diameter (SD) when rotational speed (RPM) is constant. Fig. 7 (c) shows that impact energy (IE) decreases with the increase in welding speed (WS) when shoulder diameter (SD) is constant, while impact energy (IE) increases with the increase in shoulder diameter (SD) when welding speed (WS) is constant.

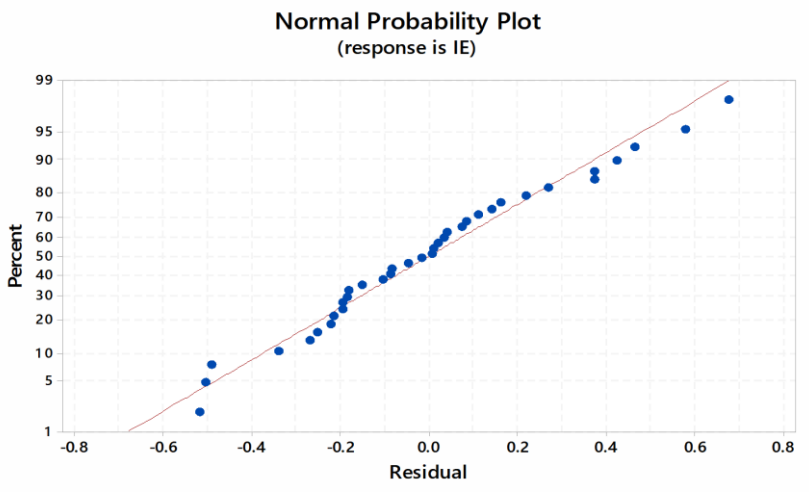

Fig. 3. Normal probability plot of IE.

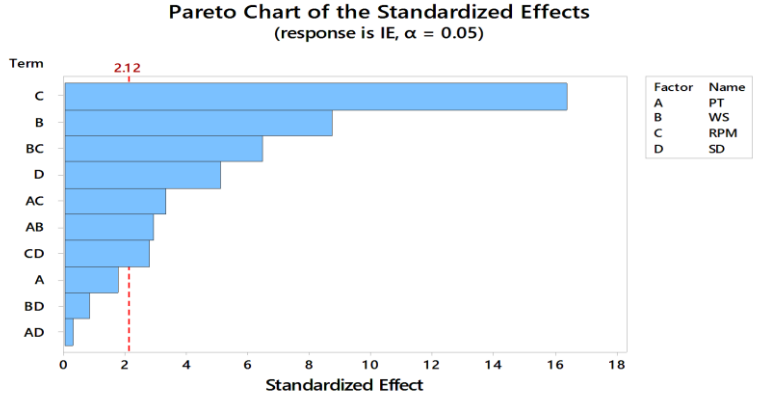

Fig. 4. Pareto Chart.

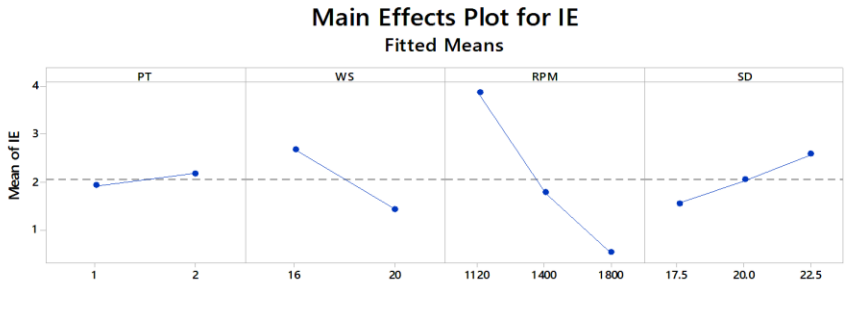

Fig. 5. Main Effect Plots.

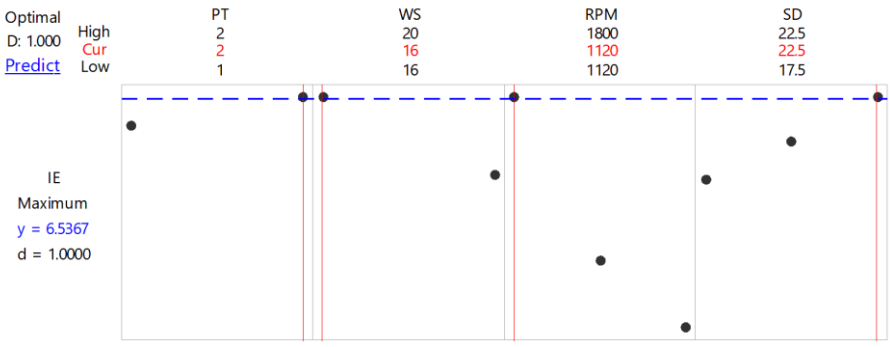

Fig. 6. Optimization Plot.

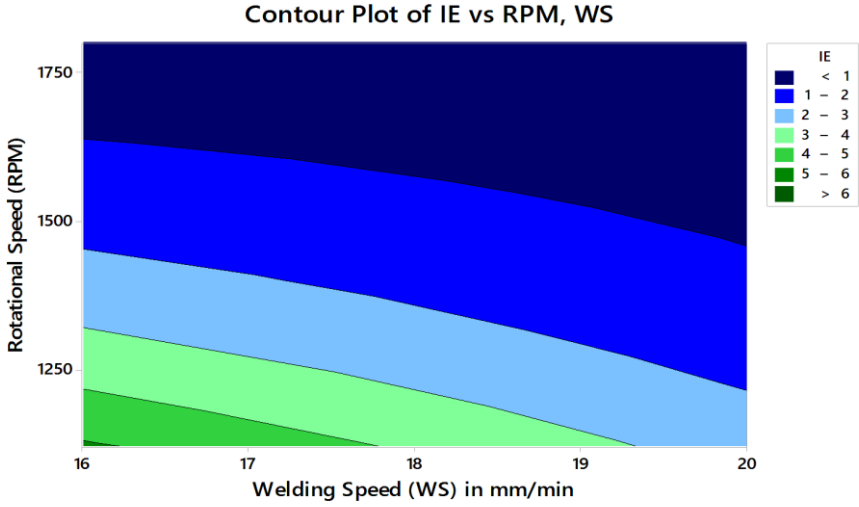

(a)

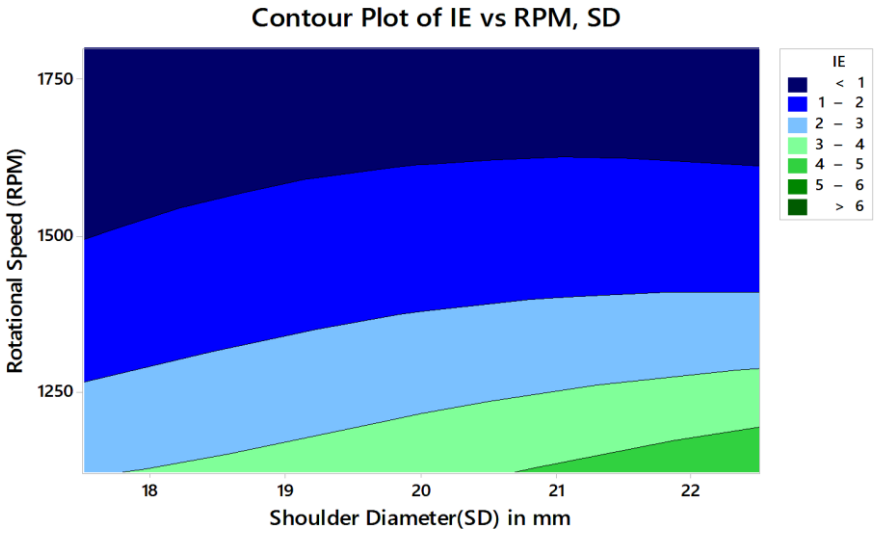

(b)

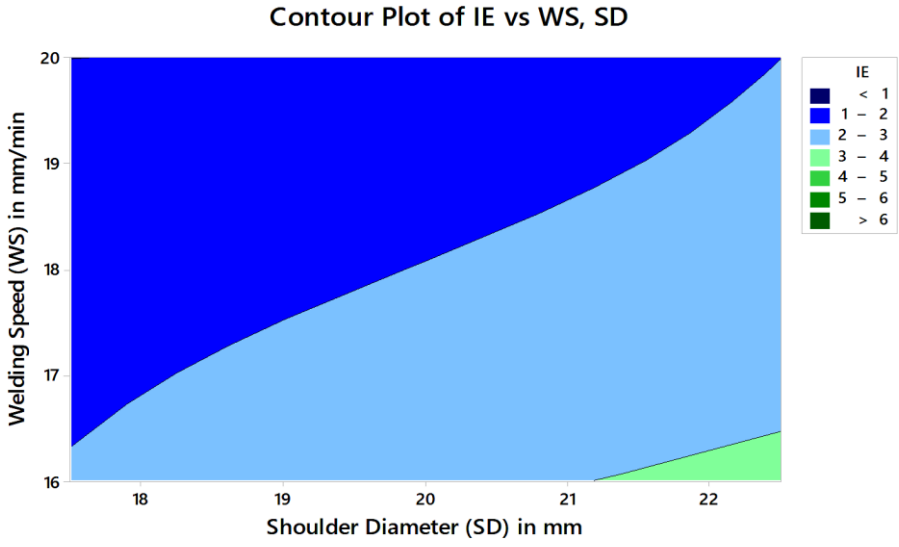

(c)

Fig. 7. Contour Plot (a) IE vs. RPM, WS (b) IE vs. RPM, SD (c) IE vs. WS, SD.

The microstructure analysis reveals grain orientation in different zones such as base metal (BM), heat affected zone (HAZ), thermo-mechanical affected zone (TMAZ), and stir zone (SZ) of weld region on the Cu side as shown in Fig. 8 (a) and the Al side as shown in Fig. 8 (b) in experiment no 21. The Cu side's base metal zone (BM) shows a twin annealed grain structure, while the base metal zone (BM) of the Al side shows an elongated grain structure. The heat-affected zone (HAZ) of Cu and Al shows distorted grain structure due to heat distribution. The thermo-mechanical affected zone (TMAZ) of Cu and Al shows grain recrystallization due to the dynamic thermo-mechanical mechanism between the tool and the workpiece. The Cu side's stir zone (SZ) shows an equiaxed grain structure, while the stir zone (SZ) of the Al side shows a fine recrystallized grain structure resulting from pin-driven material flow. The Al-Cu intermetallic compounds attribute to the maximum microhardness distribution in the stir zone (SZ). Experiment no. 21 shows a maximum microhardness of 382.24 Hv (0.1) in the stir zone (SZ), as shown in Fig. 9, owing to fine-grain recrystallization with the formation of intermetallic compounds. The microhardness of Cu's advancing side (AS) was higher than the retreating side (RS) of Al.

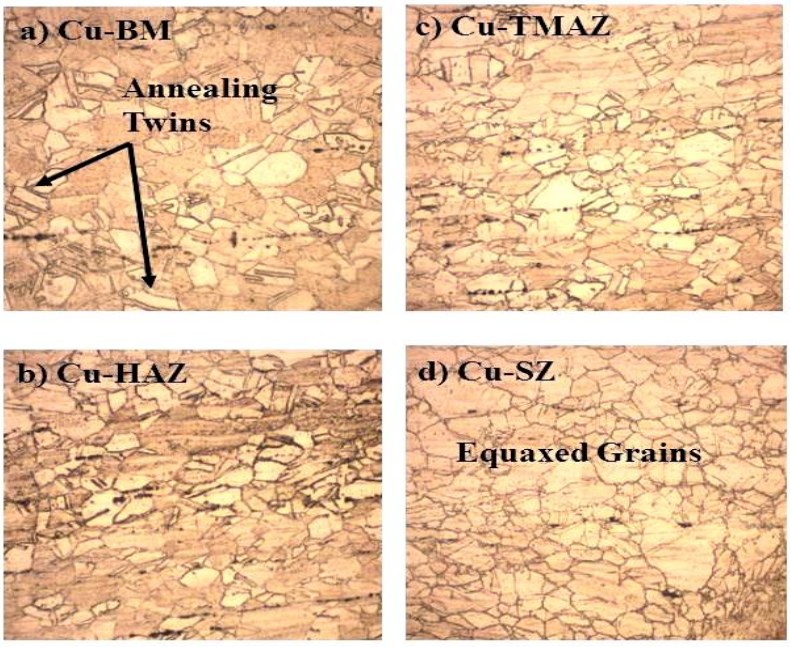

(a)

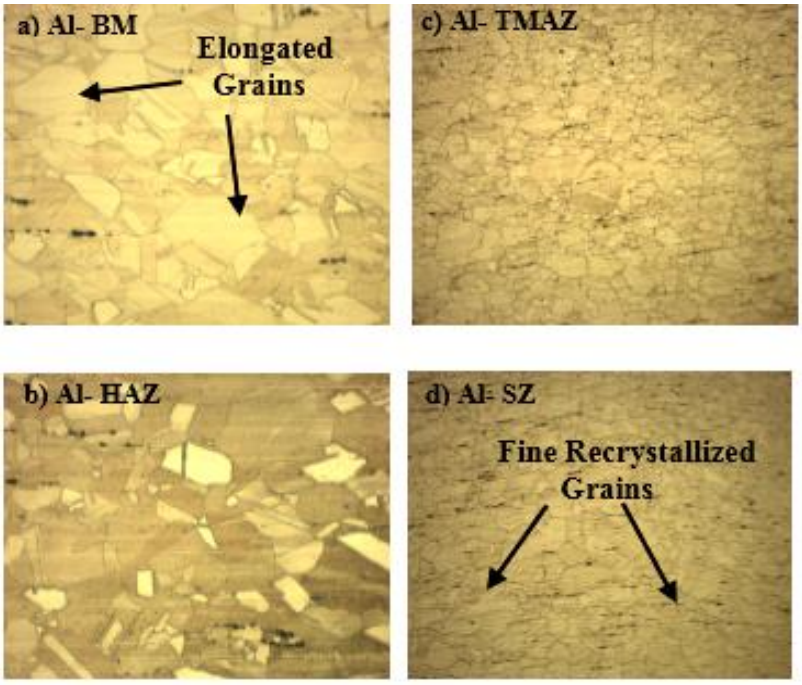

(b)

Fig. 8. Microstructure Analysis: (a) Al side, (b) Cu side.

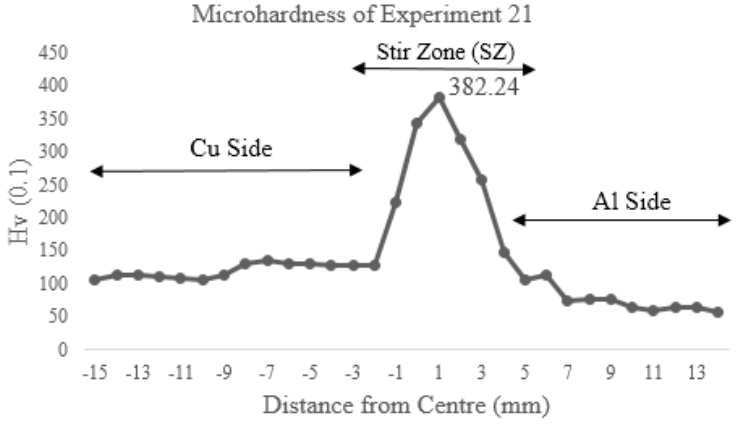

Fig. 9. Microhardness analysis.

Conclusions

The results and conclusions of this research work give critical findings as discussed below,

1. The friction stir welding of dissimilar aluminum (AA3003-H12) and Copper (C12200-H01) shows complex material flow due to differences in the physical properties of both materials.
2. The full factorial method with analysis of variance (ANOVA) gives all possible combinations of experiments with influencing process parameters affecting weld quality of a dissimilar aluminum AA3003-H12 and copper C12200-H01 weld.
3. The response optimizer tool of Minitab 18 in experiment no.21 (tapered pin, weld speed of 16 mm/min, the rotational speed of 1120 rpm, and a shoulder diameter of 22.5 mm) showed the maximum impact energy value of 6.5367 J.
4. The rotational speed is the most influencing process parameter, which has a significant influence on the impact energy of the Al-Cu weld joint with the highest value of F-ratio in the analysis of variance (ANOVA).
5. Microstructure analysis reveals that the Cu side's stir zone (SZ) shows an equiaxed grain structure. In contrast, the Al side's stir zone (SZ) offers a fine recrystallized grain structure resulting from pin-driven material flow.
6. The maximum microhardness of 382.24 Hv (0.1) was obtained in the stir zone (SZ) in experiment no. 21 (tapered pin tool, weld speed of 16 mm/min, the rotational speed of 1120 rpm, and a shoulder diameter of 22.5 mm) which is contributed to fine-grain recrystallization with the formation of Al-Cu intermetallic compounds.

Acknowledgment

The authors would like to acknowledge the Department of Mechanical Engineering, G.H. Raisoni College of Engg. and Mgmt., Pune and Shivaji University, Kolhapur for valuable support.

References

[1] Çam, V. Javaheri, A. Heidarzadeh: Journal of Adhesion Science and Technology, (2022) 1-33.

[2] Çam, G. Ipekoğlu: Int J Adv Manuf Technol, 91 (2017) 1851-1866.

[3] Çam, G. Ipekoğlu, H. Tarık Serindag: Sci. Technol. Weld Join, 19 (2014) 715-720.

[4] Küçükömeroğlu, S.M. Aktarer, G. Ipekoğlu, G. Çam: Materials Testing, 60 (2018) 1163-1170.

[5] Küçükömeroğlu, S.M. Aktarer, G. Ipekoğlu, G. Çam: International Journal of Minerals, Metallurgy and Materials, 25 (2018) 1457-1464.

[6] Çam, S. Mistikoglu, M. Pakdil: Weld J, 88 (2009) 225-232.

[7] G. Shinde, S. Gajghate, P. S. Dabeer, C. Y. Seemikeri: Materials Today: Proceedings, 4 (2017) 8901-8910.
[8] J. Ashok Raj, H.N. Shridhar Murthy, L. Arulmani, H. Santosh Kumar: Advances in Materials and Processing Technologies, (2020).
[9] W. Winarto, M. Anis, B.E. Febryansyah, In: MATEC Web of Conferences. Eds.: Anis, M., Munir, B., IIW 2018, 01001.
[10] K. P. Mehta, V. J. Badheka: Materials and Manufacturing Processes, 80 (2015) 2073-2082.
[11] N. Sharma, A.N. Siddiquee, Z.A.Khan, M.T.Mohammed: Materials and Manufacturing Processes, 33 (2017), 786-794.
[12] S. Shankar, P. Vilaça, P. Dash, S. Chattopadhyaya, S. Hloch: Measurement, 146 (2019) 892-902.
[13] P. Dabeer, G. Shinde: Materials Today: Proceedings, 5 (2018) 13166-13176.
[14] T. Chen: Journal of Materials Science, 44 (2009) 2573-2580.
[15] W. Safeen, S. Hussain, A. Wasim, M. Jahanzaib, H. Aziz, H. Abdalla: International Journal of Advanced Manufacturing Technology, 87 (2016) 1765-1781.
[16] S. Dharani Kumar, S. Senthil Kumar: Mechanics and Mechanical Engineering, 23 (2019) 59-63.
[17] A. A. Nia, A. Shirazi: International Journal of Minerals, Metallurgy, and Materials, 23 (2016) 799-809.
[18] A. K. Lakshminarayanan, V. Balasubramanian, M. Salahuddin : Journal of Iron and Steel Research International, 17 (2010) 68-74.
[19] K. Karthick, S. Malarvizhi, V. Balasubramanian, S. A. Krishnan, G. Sasikala, S. K. Albert: Nuclear Engineering and Technology, 50 (2018) 116-125.
[20] W. Zhou, K.G. Chew, H. Abdalla: Materials Science and Engineering A, 347 (2003) 180-185.
[21] L. Y. Jiang Qinglei, Wang Juan , Zhang Lei : Bull. Mater. Sci.,34 (2011) 161–167.
[22] N. K. Randy Chiong, Sumaiya Islam, Edwin Tchan: IOP Conf. Series: Materials Science and Engineering, 495 (2019) 1-9.
[23] A. Choudhary, M. Kumar, D. R. Unune: Construction and Building Materials, 228 (2019) 116725-11672.
[24] P. Yayla, E. Kaluc, K. Ural: Materials & Design, 28 (2007) 1898-1906.
[25] U. Das, V. Toppo: Mater Today: Proc, 5 (2018) 6170–6175.
[26] V. Balaguru, Balasubramanian, Visvalingam, P. Sivakumar: Journal of the Mechanical Behavior of Materials, 29 (2020) 186-194.
[27] K.G. Krishna, A. Devaraju, B. Manichandra: International Journal of Nanotechnology and Applications, 11 (2017) 285-291.
[28] J. Verma, R. Taiwade, C. Reddy, R. K. Khatirkar: Materials and Manufacturing Processes, 33 (2018) 308-314.
[29] G. Shinde, R. Arakerimath: Part E: Journal of Process Mechanical Engineering, 235 (2021) 1555-1564.
[30] A. Mahdianikhotbesara, M.H. Sehhat, M. Hadad: Metallogr Microstruct Anal, 10 (2021) 458–473.